Search for Spontaneous R-parity violation at $\sqrt{s} = 183$ GeV and 189 GeV

P. Abreu, W. Adam, T. Adye, P. Adzic, I. Azhinenko, Z. Albrecht, T. Alderweireld, G.D. Alekseev, R. Alemany, T. Allmendinger, et al.

Search for Spontaneous R-parity violation at $\sqrt{s} = 183\,\mathrm{GeV}$ and $189\,\mathrm{GeV}$

DELPHI Collaboration

Abstract

Searches for spontaneous R-parity violating signals at $\sqrt{s} = 183\,\mathrm{GeV}$ and $\sqrt{s} = 189\,\mathrm{GeV}$ have been performed using the 1997 and 1998 DELPHI data, under the assumption of R-parity breaking in the third lepton family. The expected topology for the decay of a pair of charginos into two acoplanar taus plus missing energy was investigated and no evidence for a signal was found. The results were used to derive a limit on the chargino mass and to constrain the allowed domains of the MSSM parameter space.

P.Abreu[22], W.Adam[52], T.Adye[38], P.Adzic[12], Z.Albrecht[18], T.Alderweireld[2], G.D.Alekseev[17], R.Alemany[51], T.Allmendinger[18], P.P.Allport[23], S.Almehed[25], U.Amaldi[29], N.Amapane[47], S.Amato[49], E.G.Anassontzis[3], P.Andersson[46], A.Andreazza[28], S.Andringa[22], P.Antilogus[26], W-D.Apel[18], Y.Arnoud[15], B.Åsman[46], J-E.Augustin[24], A.Augustinus[9], P.Baillon[9], A.Ballestrero[47], P.Bambade[9,20], F.Barao[22], G.Barbiellini[48], R.Barbier[26], D.Y.Bardin[17], G.Barker[18], A.Baroncelli[40], M.Battaglia[16], M.Baubillier[24], K-H.Becks[54], M.Begalli[6], A.Behrmann[54], P.Beilliere[8], Yu.Belokopytov[9], N.C.Benekos[33], A.C.Benvenuti[5], C.Berat[15], M.Berggren[24], L.Berntzon[46], D.Bertrand[2], M.Besancon[41], M.S.Bilenky[17], M-A.Bizouard[20], D.Bloch[10], H.M.Blom[32], M.Bonesini[29], M.Boonekamp[41], P.S.L.Booth[23], G.Borisov[20], C.Bosio[43], O.Botner[50], E.Boudinov[32], B.Bouquet[20], C.Bourdarios[20], T.J.V.Bowcock[23], I.Boyko[17], I.Bozovic[12], M.Bozzo[14], M.Bracko[45], P.Branchini[40], R.A.Brenner[50], P.Bruckman[9], J-M.Brunet[8], L.Bugge[34], T.Buran[34], B.Buschbeck[52], P.Buschmann[54], S.Cabrera[51], M.Caccia[28], M.Calvi[29], T.Camporesi[9], V.Canale[39], F.Carena[9], L.Carroll[23], C.Caso[14], M.V.Castillo Gimenez[51], A.Cattai[9], F.R.Cavallo[5], Ph.Charpentier[9], P.Checchia[37], G.A.Chelkov[17], R.Chierici[47], P.Chliapnikov[9,44], P.Chochula[7], V.Chorowicz[26], J.Chudoba[31], K.Cieslik[19], P.Collins[9], R.Contri[14], E.Cortina[51], G.Cosme[20], F.Cossutti[9], M.Costa[51], H.B.Crawley[1], D.Crennell[38], G.Crosetti[14], J.Cuevas Maestro[35], S.Czellar[16], J.D'Hondt[2], J.Dalmau[46], M.Davenport[9], W.Da Silva[24], G.Della Ricca[48], P.Delpierre[27], N.Demaria[47], A.De Angelis[48], W.De Boer[18], C.De Clercq[2], B.De Lotto[48], A.De Min[9], L.De Paula[49], H.Dijkstra[9], L.Di Ciaccio[39], J.Dolbeau[8], K.Doroba[53], M.Dracos[10], J.Drees[54], M.Dris[33], G.Eigen[4], T.Ekelof[50], M.Ellert[50], M.Elsing[9], J-P.Engel[10], M.Espirito Santo[9], G.Fanourakis[12], D.Fassouliotis[12], M.Feindt[18], J.Fernandez[42], A.Ferrer[51], E.Ferrer-Ribas[20], F.Ferro[14], A.Firestone[1], U.Flagmeyer[54], H.Foeth[9], E.Fokitis[33], F.Fontanelli[14], B.Franek[38], A.G.Frodesen[4], R.Fruhwirth[52], F.Fulda-Quenzer[20], J.Fuster[51], A.Galloni[23], D.Gamba[47], S.Gamblin[20], M.Gandelman[49], C.Garcia[51], C.Gaspar[9], M.Gaspar[49], U.Gasparini[37], Ph.Gavillet[9], E.N.Gazis[33], D.Gele[10], T.Geralis[12], N.Ghodbane[26], I.Gil[51], F.Glege[54], R.Gokieli[9,53], B.Golob[9,45], G.Gomez-Ceballos[42], P.Goncalves[22], I.Gonzalez Caballero[42], G.Gopal[38], L.Gorn[1], V.Gracco[14], J.Grahl[1], E.Graziani[40], P.Gris[41], G.Grosdidier[20], K.Grzelak[53], J.Guy[38], C.Haag[18], F.Hahn[9], S.Hahn[54], S.Haider[9], A.Hallgren[50], K.Hamacher[54], J.Hansen[34], F.J.Harris[36], F.Hauler[18], V.Hedberg[9,25], S.Heising[18], J.J.Hernandez[51], P.Herquet[2], H.Herr[9], E.Higon[51], S-O.Holmgren[46], P.J.Holt[36], S.Hoorelbeke[2], M.Houlden[23], J.Hrubec[52], M.Huber[18], G.J.Hughes[23], K.Hultqvist[9,46], J.N.Jackson[23], R.Jacobsson[9], P.Jalocha[19], R.Janik[7], Ch.Jarlskog[25], G.Jarlskog[25], P.Jarry[41], B.Jean-Marie[20], D.Jeans[36], E.K.Johansson[46], P.Jonsson[26], C.Joram[9], P.Juillot[10], L.Jungermann[18], F.Kapusta[24], K.Karafasoulis[12], S.Katsanevas[26], E.C.Katsoufis[33], R.Keranen[18], G.Kernel[45], B.P.Kersevan[45], B.A.Khomenko[17], N.N.Khovanski[17], A.Kiiskinen[16], B.King[23], A.Kinvig[23], N.J.Kjaer[9], O.Klapp[54], P.Kluit[32], P.Kokkinias[12], C.Kourkoumelis[3], O.Kouznetsov[17], M.Krammer[52], E.Kriznic[45], Z.Krumstein[17], P.Kubinec[7], J.Kurowska[53], K.Kurvinen[16], J.W.Lamsa[1], D.W.Lane[1], J-P.Laugier[41], R.Lauhakangas[16], G.Leder[52], F.Ledroit[15], L.Leinonen[46], A.Leisos[12], R.Leitner[31], G.Lenzen[54], V.Lepeltier[20], T.Lesiak[19], M.Lethuillier[26], J.Libby[36], W.Liebig[54], D.Liko[9], A.Lipniacka[46], I.Lippi[37], B.Loerstad[25], J.G.Loken[36], J.H.Lopes[49], J.M.Lopez[42], R.Lopez-Fernandez[15], D.Loukas[12], P.Lutz[41], L.Lyons[36], J.MacNaughton[52], J.R.Mahon[6], A.Maio[22], A.Malek[54], S.Maltezos[33], V.Malychev[17], F.Mandl[52], J.Marco[42], R.Marco[42], B.Marechal[49], M.Margoni[37], J-C.Marin[9], C.Mariotti[9], A.Markou[12], C.Martinez-Rivero[9], S.Marti i Garcia[9], J.Masik[13], N.Mastroyiannopoulos[12], F.Matorras[42], C.Matteuzzi[29], G.Matthiae[39], F.Mazzucato[37], M.Mazzucato[37], M.Mc Cubbin[23], R.Mc Kay[1], R.Mc Nulty[23], G.Mc Pherson[23], E.Merle[15], C.Meroni[28], W.T.Meyer[1], E.Migliore[9], L.Mirabito[26], W.A.Mitaroff[52], U.Mjoernmark[25], T.Moa[46], M.Moch[18], R.Moeller[30], K.Moenig[9,11], M.R.Monge[14], D.Moraes[49], P.Morettini[14], G.Morton[36], U.Mueller[54], K.Muenich[54], M.Mulders[32], C.Mulet-Marquis[15], L.M.Mundim[6], R.Muresan[25], W.J.Murray[38], B.Muryn[19], G.Myatt[36], T.Myklebust[34], F.Naraghi[15], M.Nassiakou[12], F.L.Navarria[5], K.Nawrocki[53], P.Negri[29], N.Neufeld[52], R.Nicolaidou[41], B.S.Nielsen[30], P.Niezurawski[53], M.Nikolenko[10,17], V.Nomokonov[16], A.Nygren[25], A.G.Olshevski[17], A.Onofre[22], R.Orava[16], G.Orazi[10], K.Osterberg[9], A.Ouraou[41], A.Oyanguren[51], M.Paganoni[29], S.Paiano[5], R.Pain[24], R.Paiva[22], J.Palacios[36], H.Palka[19], Th.D.Papadopoulou[33], L.Pape[9], C.Parkes[9], F.Parodi[14], U.Parzefall[23], A.Passeri[40], O.Passon[54], T.Pavel[25], M.Pegoraro[37], L.Peralta[22], M.Pernicka[52], A.Perrotta[5], C.Petridou[48], A.Petrolini[14], H.T.Phillips[38], F.Pierre[41], M.Pimenta[22], E.Piotto[28], T.Podobnik[45], V.Poireau[41], M.E.Pol[6], G.Polok[19], P.Poropat[48], V.Pozdniakov[17], P.Privitera[39], N.Pukhaeva[17], A.Pullia[29], D.Radojicic[36], S.Ragazzi[29], H.Rahmani[33], J.Rames[13], P.N.Ratoff[21], A.L.Read[34], P.Rebecchi[9], N.G.Redaelli[29], M.Regler[52], J.Rehn[18], D.Reid[32], P.Reinertsen[4], R.Reinhardt[54], P.B.Renton[36], L.K.Resvanis[3], F.Richard[20], J.Ridky[13], G.Rinaudo[47], I.Ripp-Baudot[10], A.Romero[47], P.Ronchese[37], E.I.Rosenberg[1], P.Rosinsky[7], P.Roudeau[20], T.Rovelli[5], V.Ruhlmann-Kleider[41], A.Ruiz[42], H.Saarikko[16], Y.Sacquin[41], A.Sadovsky[17], G.Sajot[15], J.Salt[51], D.Sampsonidis[12], M.Sannino[14], A.Savoy-Navarro[24], Ph.Schwemling[24], B.Schwering[54], U.Schwickerath[18], F.Scuri[48], P.Seager[21], Y.Sedykh[17], A.M.Segar[36], N.Seibert[18], R.Sekulin[38], G.Sette[14], R.C.Shellard[6], M.Siebel[54], L.Simard[41], F.Simonetto[37], A.N.Sisakian[17], G.Smadja[26], O.Smirnova[25], G.R.Smith[38], A.Sopczak[18], R.Sosnowski[53], T.Spassov[9], E.Spiriti[40], S.Squarcia[14], C.Stanescu[40], M.Stanitzki[18], K.Stevenson[36], A.Stocchi[20], J.Strauss[52], R.Strub[10], B.Stugu[4], M.Szczekowski[53], M.Szeptycka[53], T.Tabarelli[29], A.Taffard[23], F.Tegenfeldt[50], F.Terranova[29], J.Timmermans[32], N.Tinti[5], L.G.Tkatchev[17], M.Tobin[23], S.Todorova[9], B.Tome[22], A.Tonazzo[9], L.Tortora[40], P.Tortosa[51], G.Transtromer[25], D.Treille[9], G.Tristram[8], M.Trochimczuk[53], C.Troncon[28], M-L.Turluer[41], I.A.Tyapkin[17], P.Tyapkin[25], S.Tzamarias[12], O.Ullaland[9], G.Valenti[9,5], E.Vallazza[48], P.Van Dam[32], W.Van den Boeck[2], J.Van Eldik[9,32], A.Van Lysebetten[2], N.van Remortel[2], I.Van Vulpen[32], G.Vegni[28], L.Ventura[37], W.Venus[38,9],

F.Verbeure[2], P.Verdier[26], M.Verlato[37], L.S.Vertogradov[17], V.Verzi[28], D.Vilanova[41], L.Vitale[48], A.S.Vodopyanov[17], G.Voulgaris[3], V.Vrba[13], H.Wahlen[54], A.J.Washbrook[23], C.Weiser[9], D.Wicke[9], J.H.Wickens[2], G.R.Wilkinson[36], M.Winter[10], M.Witek[19], G.Wolf[9], J.Yi[1], A.Zalewska[19], P.Zalewski[53], D.Zavrtanik[45], E.Zevgolatakos[12], N.I.Zimin[17,25], A.Zintchenko[17], Ph.Zoller[10], G.Zumerle[37], M.Zupan[12]

[1]Department of Physics and Astronomy, Iowa State University, Ames IA 50011-3160, USA
[2]Physics Department, Univ. Instelling Antwerpen, Universiteitsplein 1, B-2610 Antwerpen, Belgium
 and IIHE, ULB-VUB, Pleinlaan 2, B-1050 Brussels, Belgium
 and Faculté des Sciences, Univ. de l'Etat Mons, Av. Maistriau 19, B-7000 Mons, Belgium
[3]Physics Laboratory, University of Athens, Solonos Str. 104, GR-10680 Athens, Greece
[4]Department of Physics, University of Bergen, Allégaten 55, NO-5007 Bergen, Norway
[5]Dipartimento di Fisica, Università di Bologna and INFN, Via Irnerio 46, IT-40126 Bologna, Italy
[6]Centro Brasileiro de Pesquisas Físicas, rua Xavier Sigaud 150, BR-22290 Rio de Janeiro, Brazil
 and Depto. de Física, Pont. Univ. Católica, C.P. 38071 BR-22453 Rio de Janeiro, Brazil
 and Inst. de Física, Univ. Estadual do Rio de Janeiro, rua São Francisco Xavier 524, Rio de Janeiro, Brazil
[7]Comenius University, Faculty of Mathematics and Physics, Mlynska Dolina, SK-84215 Bratislava, Slovakia
[8]Collège de France, Lab. de Physique Corpusculaire, IN2P3-CNRS, FR-75231 Paris Cedex 05, France
[9]CERN, CH-1211 Geneva 23, Switzerland
[10]Institut de Recherches Subatomiques, IN2P3 - CNRS/ULP - BP20, FR-67037 Strasbourg Cedex, France
[11]Now at DESY-Zeuthen, Platanenallee 6, D-15735 Zeuthen, Germany
[12]Institute of Nuclear Physics, N.C.S.R. Demokritos, P.O. Box 60228, GR-15310 Athens, Greece
[13]FZU, Inst. of Phys. of the C.A.S. High Energy Physics Division, Na Slovance 2, CZ-180 40, Praha 8, Czech Republic
[14]Dipartimento di Fisica, Università di Genova and INFN, Via Dodecaneso 33, IT-16146 Genova, Italy
[15]Institut des Sciences Nucléaires, IN2P3-CNRS, Université de Grenoble 1, FR-38026 Grenoble Cedex, France
[16]Helsinki Institute of Physics, HIP, P.O. Box 9, FI-00014 Helsinki, Finland
[17]Joint Institute for Nuclear Research, Dubna, Head Post Office, P.O. Box 79, RU-101 000 Moscow, Russian Federation
[18]Institut für Experimentelle Kernphysik, Universität Karlsruhe, Postfach 6980, DE-76128 Karlsruhe, Germany
[19]Institute of Nuclear Physics and University of Mining and Metalurgy, Ul. Kawiory 26a, PL-30055 Krakow, Poland
[20]Université de Paris-Sud, Lab. de l'Accélérateur Linéaire, IN2P3-CNRS, Bât. 200, FR-91405 Orsay Cedex, France
[21]School of Physics and Chemistry, University of Lancaster, Lancaster LA1 4YB, UK
[22]LIP, IST, FCUL - Av. Elias Garcia, 14-1°, PT-1000 Lisboa Codex, Portugal
[23]Department of Physics, University of Liverpool, P.O. Box 147, Liverpool L69 3BX, UK
[24]LPNHE, IN2P3-CNRS, Univ. Paris VI et VII, Tour 33 (RdC), 4 place Jussieu, FR-75252 Paris Cedex 05, France
[25]Department of Physics, University of Lund, Sölvegatan 14, SE-223 63 Lund, Sweden
[26]Université Claude Bernard de Lyon, IPNL, IN2P3-CNRS, FR-69622 Villeurbanne Cedex, France
[27]Univ. d'Aix - Marseille II - CPP, IN2P3-CNRS, FR-13288 Marseille Cedex 09, France
[28]Dipartimento di Fisica, Università di Milano and INFN-MILANO, Via Celoria 16, IT-20133 Milan, Italy
[29]Dipartimento di Fisica, Univ. di Milano-Bicocca and INFN-MILANO, Piazza delle Scienze 2, IT-20126 Milan, Italy
[30]Niels Bohr Institute, Blegdamsvej 17, DK-2100 Copenhagen Ø, Denmark
[31]IPNP of MFF, Charles Univ., Areal MFF, V Holesovickach 2, CZ-180 00, Praha 8, Czech Republic
[32]NIKHEF, Postbus 41882, NL-1009 DB Amsterdam, The Netherlands
[33]National Technical University, Physics Department, Zografou Campus, GR-15773 Athens, Greece
[34]Physics Department, University of Oslo, Blindern, NO-1000 Oslo 3, Norway
[35]Dpto. Fisica, Univ. Oviedo, Avda. Calvo Sotelo s/n, ES-33007 Oviedo, Spain
[36]Department of Physics, University of Oxford, Keble Road, Oxford OX1 3RH, UK
[37]Dipartimento di Fisica, Università di Padova and INFN, Via Marzolo 8, IT-35131 Padua, Italy
[38]Rutherford Appleton Laboratory, Chilton, Didcot OX11 OQX, UK
[39]Dipartimento di Fisica, Università di Roma II and INFN, Tor Vergata, IT-00173 Rome, Italy
[40]Dipartimento di Fisica, Università di Roma III and INFN, Via della Vasca Navale 84, IT-00146 Rome, Italy
[41]DAPNIA/Service de Physique des Particules, CEA-Saclay, FR-91191 Gif-sur-Yvette Cedex, France
[42]Instituto de Fisica de Cantabria (CSIC-UC), Avda. los Castros s/n, ES-39006 Santander, Spain
[43]Dipartimento di Fisica, Università degli Studi di Roma La Sapienza, Piazzale Aldo Moro 2, IT-00185 Rome, Italy
[44]Inst. for High Energy Physics, Serpukov P.O. Box 35, Protvino, (Moscow Region), Russian Federation
[45]J. Stefan Institute, Jamova 39, SI-1000 Ljubljana, Slovenia and Laboratory for Astroparticle Physics,
 Nova Gorica Polytechnic, Kostanjeviska 16a, SI-5000 Nova Gorica, Slovenia,
 and Department of Physics, University of Ljubljana, SI-1000 Ljubljana, Slovenia
[46]Fysikum, Stockholm University, Box 6730, SE-113 85 Stockholm, Sweden
[47]Dipartimento di Fisica Sperimentale, Università di Torino and INFN, Via P. Giuria 1, IT-10125 Turin, Italy
[48]Dipartimento di Fisica, Università di Trieste and INFN, Via A. Valerio 2, IT-34127 Trieste, Italy
 and Istituto di Fisica, Università di Udine, IT-33100 Udine, Italy
[49]Univ. Federal do Rio de Janeiro, C.P. 68528 Cidade Univ., Ilha do Fundão BR-21945-970 Rio de Janeiro, Brazil
[50]Department of Radiation Sciences, University of Uppsala, P.O. Box 535, SE-751 21 Uppsala, Sweden
[51]IFIC, Valencia-CSIC, and D.F.A.M.N., U. de Valencia, Avda. Dr. Moliner 50, ES-46100 Burjassot (Valencia), Spain
[52]Institut für Hochenergiephysik, Österr. Akad. d. Wissensch., Nikolsdorfergasse 18, AT-1050 Vienna, Austria
[53]Inst. Nuclear Studies and University of Warsaw, Ul. Hoza 69, PL-00681 Warsaw, Poland
[54]Fachbereich Physik, University of Wuppertal, Postfach 100 127, DE-42097 Wuppertal, Germany

1 Introduction

R-parity is a discrete symmetry assigned as $R_p = (-1)^{3B+L+2S}$, where B is the baryon number, L is the lepton number and S is the particle spin. In the Minimal Supersymmetric Standard Model (MSSM) the R-parity symmetry is assumed to be conserved [1]. Under this assumption the supersymmetric particles must be produced in pairs, every SUSY particle decays into another SUSY particle and the lightest of them is absolutely stable. These features underly most of the experimental searches for supersymmetric states.

One alternative supersymmetric scenario is to consider the R-parity as an exact Lagrangian symmetry, broken spontaneously through the Higgs mechanism [2]. This may take place via non-zero vacuum expectation values (VEVs) for scalar neutrinos, such as for the scalar tau-neutrinos

$$v_R = \langle \tilde{\nu}_{R\tau} \rangle \ ; \quad v_L = \langle \tilde{\nu}_{L\tau} \rangle \ . \tag{1}$$

In this case there are two main scenarios depending on whether the lepton number is a gauge symmetry or not [3–7]. In the absence of an additional gauge symmetry, it leads to the existence of a physical massless Nambu-Goldstone boson, called the Majoron (J) [4]. In this context the Majoron remains massless and therefore stable provided that there are no explicit R-parity violating terms.

1.1 Spontaneous R-Parity violation

In the present work we consider the simplest version of the R-parity spontaneous violation model described in Ref. [4,5]. In this model the Lagrangian is specified by the superpotential

$$W = W_1 + h_\nu \nu^c L H_u + h \Phi \nu^c S + h.c. \tag{2}$$

that conserves the total lepton number and R-parity. The first part of this equation contains the basic MSSM superpotential terms, including an isosinglet scalar Φ with a linear superpotential coupling, written as:

$$W_1 = h_u Q u^c H_u + h_d Q d^c H_d + h_e e^c L H_d + (h_0 H_u H_d - \mu'^2) \Phi \ . \tag{3}$$

The couplings h_u, h_d, h_e, h_ν, h_0, h are described by arbitrary matrices in the generation space and explicitly break flavour conservation. The additional chiral superfields ν^c, S [8] and Φ [9] are singlets under $SU(2) \otimes U(1)$ and carry a conserved lepton number assigned as -1, 1 and 0, respectively. These superfields may induce the spontaneous violation of R-parity, given by the imaginary part of:

$$\frac{v_L^2}{V v^2}(v_u H_u - v_d H_d) + \frac{v_L}{V}\tilde{\nu}_\tau - \frac{v_R}{V}\tilde{\nu}_\tau^c + \frac{v_S}{V}\tilde{S}_\tau \ , \tag{4}$$

leading to an R-odd Majoron. The isosinglet VEVs $v_R = \langle \tilde{\nu}_{R\tau} \rangle$ and $v_S = \langle \tilde{S}_\tau \rangle$, with $V = \sqrt{v_R^2 + v_S^2}$, characterise the R-parity breaking and the isodoublet VEVs $v_u = \langle H_u \rangle$, $v_d = \langle H_d \rangle$ and $v_L = \langle \tilde{\nu}_{L\tau} \rangle$ induce the electroweak breaking and generate the fermion masses. For theoretical reasons the R-parity breaking was introduced only in the third family, since the largest Yukawa couplings are those of the third generation. In that case the R-parity breaking is effectively parameterised by a bilinear superpotential term given by:

$$\epsilon_i \equiv h_{\nu_{i3}} v_{R3} \ . \tag{5}$$

This effective parameter leads to the R-parity violating gauge couplings and contributes to the mixing between the charged (neutral) leptons and the charginos (neutralinos), as can be seen from the fermion mass matrices in Ref. [10].

By construction, neutrinos are massless at the Lagrangian level but get mass from the mixing with neutralinos [6,10]. As a result, all R-parity violating observables are directly correlated to the τ neutrino mass:

$$m_{\nu_\tau} \sim \frac{\xi \epsilon^2}{m_{\tilde{\chi}}} , \tag{6}$$

where $m_{\tilde{\chi}}$ is the neutralino mass, ϵ is the R-parity violation parameter and ξ is an effective parameter [11] given as a function of M_2, μ and $\tan\beta$.

1.2   Chargino Decay Modes

At LEP2 the chargino can be pair produced from e^+e^- via exchange of γ, Z or $\tilde{\nu}$. In the present analysis it is assumed that all sfermions are sufficiently heavy ($M_{\tilde{\nu}} \geq 300\,\text{GeV}/c^2$) not to influence the chargino production or decay. Therefore, only the γ and Z s-channels contribute to the chargino cross-section. In the spontaneous R-parity violation model with R-parity breaking in the third generation, the lightest chargino ($\tilde{\chi}^\pm$) can undergo a two-body decay mode with a Majoron (J) in the final state

$$\tilde{\chi}^\pm \to \tau^\pm J \tag{7}$$

in addition to the "conventional" chargino channels

$$\tilde{\chi}^\pm \to \nu_\tau W^\pm \to \nu_\tau q\bar{q}', \ \nu_\tau l_i^\pm \nu_i \tag{8}$$

and

$$\tilde{\chi}^\pm \to \tilde{\chi}^0 W^\pm \to \tilde{\chi}^0 q\bar{q}', \ \tilde{\chi}^0 l_i^\pm \nu_i . \tag{9}$$

Both the two-body decay (7) and the decay with a neutralino in the final state (9) are R-parity conserving, while in equation (8) the chargino decays through an R-parity violating vertex. The decay branching ratios depend strongly on the effective R-parity violation parameter (ϵ), as can be observed in figure 1. Note that in a large range of ϵ the new two-body decay mode is the dominant channel and, since it is R-parity conserving, it can be large.

1.3   Parameter Values

All the results discussed in the following sections were achieved by assuming that the chargino decays mainly via the new two body decay mode, described in equation (7). As was already mentioned, all sfermions are considered to be sufficiently heavy ($M_{\tilde{\nu}} \geq 300\,\text{GeV}/c^2$) not to influence the chargino production or decay. Typical ranges of values for the SUSY parameters $\mu \equiv h_0\langle\Phi\rangle$ and M_2 are assumed:

$$-200\,\text{GeV}/c^2 \leq \mu \leq 200\,\text{GeV}/c^2 \tag{10}$$

$$40\,\text{GeV}/c^2 \leq M_2 \leq 400\,\text{GeV}/c^2 , \tag{11}$$

which can be covered by the chargino production at LEP. Also assumed are the GUT relation $M_1/M_2 = 5/3 \tan^2\theta_W$ and that $\tan\beta$ ($= v_u/v_d$) lies in the range

$$2 \leq \tan\beta \leq 40 . \tag{12}$$

2 Detector Description

The following is a summary of the properties of the DELPHI detector [12] relevant to this analysis. Charged particle tracks were reconstructed in the 1.2 T solenoidal magnetic field by a system of cylindrical tracking detectors. These were the microVertex Detector (VD), the Inner Detector (ID), the Time Projection Chamber (TPC), and the Outer Detector (OD). In addition, two planes of drift chambers aligned perpendicular to the beam axis (Forward Chambers A and B) tracked particles in the forward and backward directions, covering polar angles $11° < \theta < 33°$ and $147° < \theta < 169°$ with respect to the beam (z) direction.

The VD consisted of three cylindrical layers of silicon detectors, at radii 6.3 cm, 9.0 cm and 11.0 cm. All three layers measured coordinates in the plane transverse to the beam. The closest (6.3 cm) and the outer (11.0 cm) layers contained double-sided detectors to measure also z coordinates. The polar angle coverage of the VD was from 25° to 155°. Mini-strips and pixel detectors making up the Very Forward Tracker (VFT) have been added to the ends of the VD increasing the angular acceptance to include the regions from 10° to 25° and from 155° to 170° [13]. The ID, covering polar angles between 15° and 165°, was composed of a cylindrical drift chamber (inner radius 12 cm and outer radius 22 cm) surrounded by 5 layers of straw drift tubes with inner radius of 23 cm and outer radius of 28 cm. The TPC, the principal tracking device of DELPHI, was a cylinder of 30 cm inner radius, 122 cm outer radius and length 2.7 m. Each end-plate was divided into 6 sectors, with 192 sense wires and 16 circular pad rows used for 3 dimensional space-point reconstruction. The OD consisted of 5 layers of drift cells at radii between 198 cm and 206 cm, covering polar angles between 43° and 137°.

The average momentum resolution for the charged particles in hadronic final states was in the range $\Delta p/p^2 \simeq 0.001$ to 0.01 $(\text{GeV}/c)^{-1}$, depending on which detectors were used in the track fit [12].

The electromagnetic calorimeters were the High density Projection Chamber (HPC) covering the barrel region of $40° < \theta < 140°$, the Forward ElectroMagnetic Calorimeter (FEMC) covering $11° < \theta < 36°$ and $144° < \theta < 169°$, and the STIC, a Scintillator TIle Calorimeter which extended coverage down to 1.66° from the beam axis in either direction. The 40° taggers were a series of single layer scintillator-lead counters used to veto electromagnetic particles that would otherwise have been missed in the region between the HPC and FEMC. A similar set of taggers was arranged at 90° to cover the gap between the two halves of the HPC. The efficiency to register a photon with energy above 5 GeV, measured with the LEP1 data, was above 99%. The hadron calorimeter (HCAL) covered 98% of the solid angle. Muons with momenta above 2 GeV/c penetrated the HCAL and were recorded in a set of muon drift chambers.

3 Data Samples

The data collected by the DELPHI detector during 1997 at $\sqrt{s} \simeq 183$ GeV and 1998 at $\sqrt{s} \simeq 189$ GeV, corresponding to integrated luminosities of $53\,\text{pb}^{-1}$ and $158\,\text{pb}^{-1}$ respectively, were analysed.

To evaluate background contaminations, different contributions from the Standard Model processes were considered. The background processes WW, W$e\nu_e$, ZZ, Ze^+e^- and Z/$\gamma \rightarrow q\bar{q}(\gamma)$ were generated using PYTHIA [14], while the events Z/$\gamma \rightarrow \tau^+\tau^-(\gamma), \mu^+\mu^-(\gamma)$ were produced by KORALZ [15] and DYMU3 [16] respectively. A cross-check was performed using the four-fermion final states generated with EXCAL-

IBUR [17]. The generator BABAMC [18] was used for the Bhabha scattering. Two-photon interactions leading to leptonic and hadronic final states were produced by the BDK [19] and TWOGAM [20] programs, respectively. All the background events were passed through a detailed detector response simulation (DELSIM) and reconstructed as the real data [12].

The program RP-generator II, described in reference [5], was used to calculate the masses, production cross-sections and decay branching ratios of the chargino. The chargino pair production was considered for different values of the R-parity violation parameter (ϵ) and at several points of the MSSM parameter space ($\tan\beta, \mu, M_2$). For the signal, a faster simulation program SGV[1] was used to check the points that were not generated by the full DELPHI simulation program (DELSIM). The SGV program does not simulate the DELPHI taggers. To correct for this effect, ten chargino mass points, with 1000 events each, were simulated by DELSIM and the selection efficiencies[2] calculated from the two simulations were compared. Any differences between the two were used as a correction factor, shown in figure 2.

4 Chargino Searches

With the R-parity spontaneous breaking, the chargino can decay through an R-parity conserving vertex into $\tau^\pm J$ events. Due to the undetectable Majoron, such events have the topology of two taus acoplanar with the beam axis plus missing energy. To select events with this signature it was required that the charged and neutral particles were well reconstructed and that the total momentum transverse to the beam was greater than $4\,\mathrm{GeV/c}$. A particle was considered as well reconstructed if it had a momentum between $1\,\mathrm{GeV/c}$ and the beam momentum and a polar angle between $30°$ and $150°$. As a result 4006 events at $183\,\mathrm{GeV}$ and 11350 at $189\,\mathrm{GeV}$ were selected. The efficiency of detecting signal events at this level of selection was around $47\,\%$. The simulated remaining backgrounds are detailed in table 1.

Events were also required to have less than 7 charged particles and no signal in the $40°$ or $90°$ taggers. It was further required that the events consisted of two clusters of charged and neutral particles, each cluster with invariant mass below $5.5\,\mathrm{GeV/c^2}$ and with an acoplanarity[3] between $5°$ and $176°$. The clusters were constructed by considering all combinations of assigning the charged particles in the event into two groups. Neutral particles were then added to the groups such that the mass remains below the cut value and a neutral that can not be added to either of the two groups is considered as isolated.

Events with forward going secondaries were avoided by rejecting any with energy measured in a $30°$ cone around the beam axis. Some of the energy in the forward cone resulted from noise and other backgrounds which were not included in the simulation of the signal. It was estimated that $\sim 20\%$ of any signal would be rejected by this selection and the efficiency was appropriately corrected. This preliminary selection resulted in 152 observed events at $183\,\mathrm{GeV}$ and 415 at $189\,\mathrm{GeV}$, as shown in table 1, with a typical efficiency for the signal of $\sim 37\,\%$.

---

[1]The program "Simulation a Grande Vitesse" (SGV) is described in http://delphiwww.cern.ch/~berggren/sgv.html

[2]The efficiency of the chargino selection is defined as the number of events satisfying the cuts defined in Secion 4.1 divided by the total number of generated chargino events.

[3]The acoplanarity is defined as the complement of the angle between the clusters when projected onto the plane perpendicular to the beam.

4.1 Event Selection at 183 GeV

To reject the radiative return to the Z background, no events with isolated photons with more than 5 GeV were accepted. The $\gamma\gamma$ and $\mu^+\mu^-(\gamma)$ backgrounds were reduced by requiring that the events had at least one charged particle with momentum between 5 GeV/c and 60 GeV/c. To reduce the $\tau^+\tau^-(\gamma)$ background the square of transverse momentum with respect to the thrust axis divided by the thrust had to be above $0.75\,(\text{GeV}/c)^2$.

To reduce the $\gamma\gamma$ background further, events with momentum of their most energetic charged particle (P_{max}) below 10 GeV/c had to have total momentum transverse to the beam above 10.5 GeV/c. For events with $P_{max} > 10$ GeV/c, the main remaining contamination comes from $Z/\gamma \to \tau^+\tau^-$ and WW. For those, if the acoplanarity was below 15°, the angle between the missing momentum and the beam had to be greater than 30°. On the other hand, if the acoplanarity was above 15°, it was required that the momentum of the most energetic particle was below 23.5 GeV/c and the angle between the missing momentum and the beam was greater than 34.5°.

Figures 3a and 3b show the agreement between data and simulated background events after a preliminary selection, while figure 4a shows the dependence of the signal detection efficiency on the chargino mass. The selection criteria result in 6 observed events detected with a signal detection efficiency of around 18 %.

4.2 Event Selection at 189 GeV

Since LEP delivered a higher luminosity for this energy and the WW background increased, tighter cuts were applied. The required acoplanarity had to be between 10° and 176° and no events with an isolated photon were accepted. The momentum of each of the two particle clusters had to be above 5 GeV/c and below 55 GeV/c and the square of transverse momentum with respect to the thrust axis divided by the thrust had to be above $1.0\,(\text{GeV}/c)^2$. All the events had to have the angle between the missing momentum and the beam greater than 35°.

The $\gamma\gamma$ background was mainly reduced by requiring a total momentum transverse to the beam greater than 9 GeV/c. Events from WW processes were reduced by requiring that the momentum of the most energetic particle was below 23 GeV/c.

If one cluster had a momentum above 10 GeV/c and the acoplanarity was less than 15° it was also required that the value of the effective centre-of-mass energy after any initial state radiation ($\sqrt{s'}$) [21] did not fall in the region between 90 GeV and 94 GeV. For an acoplanarity above 15°, the angle between the missing momentum and the beam was required to be greater than 40° and the visible mass lower than 70 GeV/c².

Figure 3c and 3d show the agreement between data and simulated background events after a preliminary selection, while figure 4b shows the dependence of the signal detection efficiency on the chargino mass. The selection criteria result in 9 observed events with a signal detection efficiency of around 14 %.

5 Results

As a result of the selection procedure, 6 candidates of $\tilde{\chi}^\pm \to \tau^\pm + J$ were selected at 183 GeV, with a background estimation of 6.3 ± 0.4. At 189 GeV, 9 candidates were found, with an expected background of 9.6 ± 0.4. Table 1 summarises the number of accepted events in the data, together with the predicted number of events from background

sources. The systematic and statistical errors on the simulated background calculation are insignificant compared to the experimental statistical accuracy.

Assuming the chargino decays exclusively to $\tau^{\pm}J$, the data at 183 GeV and 189 GeV were combined and the standard procedure described in [22] was used to obtain a 95% confidence level upper limit on the allowed cross-section and a corresponding lower limit on the chargino mass; both are shown in figure 5. The excluded domains of the MSSM parameter space for $\tan\beta = 2$ and $\tan\beta = 40$ are shown in figure 6. The limit obtained with this $\tilde{\chi}^{\pm} \to \tau^{\pm}J$ search substantially extends the limit derived from the Z^0 line shape measured at LEP1 [23].

6 Conclusion

Searches for spontaneous R-parity violating signals used a data sample of about $211\,\mathrm{pb}^{-1}$ collected by the DELPHI detector during 1997 and 1998 at centre-of-mass energies of 183 GeV and 189 GeV. In the present analysis it was assumed that the R-parity breaking occurs in the third generation and, as a consequence, the lightest chargino decays mainly through the two-body decay mode $\tilde{\chi}^{\pm} \to \tau^{\pm} + J$. No evidence for R-parity spontaneously breaking has been observed, assuming a sneutrino mass above $300\,\mathrm{GeV/c^2}$.

In the search for $\tilde{\chi}^{\pm} \to \tau^{\pm} + J$, 15 candidates were selected, with 15.9 ± 0.6 expected from SM processes. This allowed an upper limit on the chargino production cross-section of $0.3\,\mathrm{pb}$ and a lower limit on the chargino mass of $94.3\,\mathrm{GeV/c^2}$ to be obtained at 95% confidence level. The limit obtained with the present search substantially extends the general LEP1 limit [23].

7 Acknowledgements

References

[1] H.P. Nilles, Phys. Rep. **110** (1984) 1;
    H.E. Haber and G.L. Kane, Phys. Rep. **117** (1985) 75.

[2] C.S. Aulakh, R.N. Mohapatra, Phys. Lett. **B119** (1982) 136;
    A. Santamaria, J.W.F. Valle, Phys. Lett. **B195** (1987) 423; Phys. Rev. Lett. **60** (1988) 397; Phys. Rev. **D39** (1989) 1780.

[3] J.W.F. Valle, Phys. Lett. **B196** (1987) 157;
    M.C. Gonzalez-Garcia and J.W.F. Valle, Nucl. Phys. **B355** (1991) 330.

[4] A. Masiero and J.W.F. Valle, Phys. Lett. **B251** (1990) 273;
    J.C. Romão, C.A. Santos and J.W.F. Valle, Phys. Lett. **B288** (1992) 311.

[5] F. de Campos, O.J.P. Éboli, M.A. García-Jareño, J.W.F. Valle, Nucl. Phys. **B546** (1999) 33.

[6] P. Nogueira, J.C. Romão, J.W.F. Valle, Phys. Lett. **B251** (1990) 142;
    R. Barbieri, D.E. Brahm, J. Hall, S.D.H. Hsu, Phys. Lett. **B238** (1990) 86.

[7] J.C. Romão, J. Rosiek and J.W.F. Valle, Phys. Lett. **B351** (1995) 497;
    J.C. Romão, N. Rius and J.W.F. Valle, Nucl. Phys. **B363** (1991) 369.

[8] R.N. Mohapatra and J.W.F. Valle, Phys. Rev. **D34** (1986) 1642;
    J.W.F. Valle, Nucl. Phys. **B11**(Proc. Suppl.) (1989) 118.

[9] R. Barbieri, S. Ferrara and C.A. Savoy, Phys. Lett. **B119** (1982) 343.

[10] J.C. Romão and J.W.F. Valle, Phys. Lett. **B272** (1991) 436, Nucl. Phys. **B381** (1992) 87.

[11] J.C. Romão, A. Ioannissyan and J.W.F. Valle, Phys. Rev. **D55** (1997) 427;
     M.A. Diaz, J.C. Romão and J.W.F. Valle, Nucl. Phys. **B524** (1998) 23.

[12] DELPHI Collaboration, P.Aarnio *et al.*, Nucl. Instr. and Meth. **A303** (1991) 233;
     DELPHI Collaboration, P.Abreu *et al.*, Nucl. Instr. and Meth. **A378** (1996) 57.

[13] P. Chochula et al., Nucl. Instr. and Meth. **A412** (1998) 304.

[14] T. Sjöstrand, Computer Physics Communications **39** (1986) 347.

[15] S. Jadach, B.F.L. Ward and Z. Was, Computer Physics Communications **79** (1994) 503.

[16] J.E. Campagne and R. Zitoun, Zeit. Phys. **C43** (1989) 469.

[17] F.A. Berends, R. Pittau, R. Kleiss, Computer Physics Communications **85** (1995) 437.

[18] M. Böhm, A. Denner and W. Hollik, Nucl. Phys. **B304** (1988) 687;
     F.A. Berends, R. Kleiss and W. Hollik, Nucl. Phys. **B304** (1988) 712.

[19] F.A. Berends, P.H. Daverveldt, R. Kleiss, Computer Physics Communications **40** (1986) 271, 285, 309.

[20] T. Alderweireld et al., CERN-OPEN-2000-141.

[21] DELPHI Collaboration, P.Abreu *et al.*, Phys. Lett. **B372** (1996) 172.

[22] Particle Data Group, R.M. Barnett *et al.*, Phys. Rev. **D54** (1996).

[23] L3 Collaboration, M. Acciarri *et al.*, Phys. Lett. **B350** (1995) 109;
     OPAL Collaboration, G. Alexander *et al.*, Phys. Lett. **B377** (1996) 273.

Centre-of-mass Energy	183 GeV	189 GeV
Well reconstructed charged and neutral particles		
Observed events	**4006**	**11350**
Total Expected Background	**3769 ± 7**	**11511 ± 16**
Bhabha scattering and $Z/\gamma \to ee, \mu\mu, \tau\tau, q\bar{q}$	3241 ± 4	9858 ± 2
4-fermion events except WW	14 ± 1	82 ± 2
$\gamma\gamma \to ee, \mu\mu, \tau\tau$	458 ± 5	1393 ± 16
W^+W^-	56 ± 1	178 ± 2
Preselection		
Observed events	**152**	**415**
Total Expected Background	**158 ± 4**	**494 ± 9**
Bhabha scattering and $Z/\gamma \to ee, \mu\mu, \tau\tau, q\bar{q}$	65 ± 3	207 ± 6
4-fermion events except WW	3 ± 1	10 ± 1
$\gamma\gamma \to ee, \mu\mu, \tau\tau$	53 ± 2	158 ± 7
W^+W^-	37 ± 1	119 ± 2
Final Selection		
Observed events	**6**	**9**
Total background	**6.3 ± 0.4**	**9.6 ± 0.4**
Bhabha scattering and $Z/\gamma \to ee, \mu\mu, \tau\tau, q\bar{q}$	1.0 ± 0.3	0.6 ± 0.1
4-fermion events except WW	0.6 ± 0.1	1.2 ± 0.2
$\gamma\gamma \to ee, \mu\mu, \tau\tau$	0.3 ± 0.1	0.2 ± 0.2
W^+W^-	4.4 ± 0.3	7.6 ± 0.3

Table 1: Observed events (first row of each part) and the expected backgrounds (second to sixth row) at centre-of-mass energies of 183 GeV and 189 GeV. The preselection corresponds to the selection criteria described in the introduction of Section 4. The errors quoted on the background correspond to the statistical uncertainties.
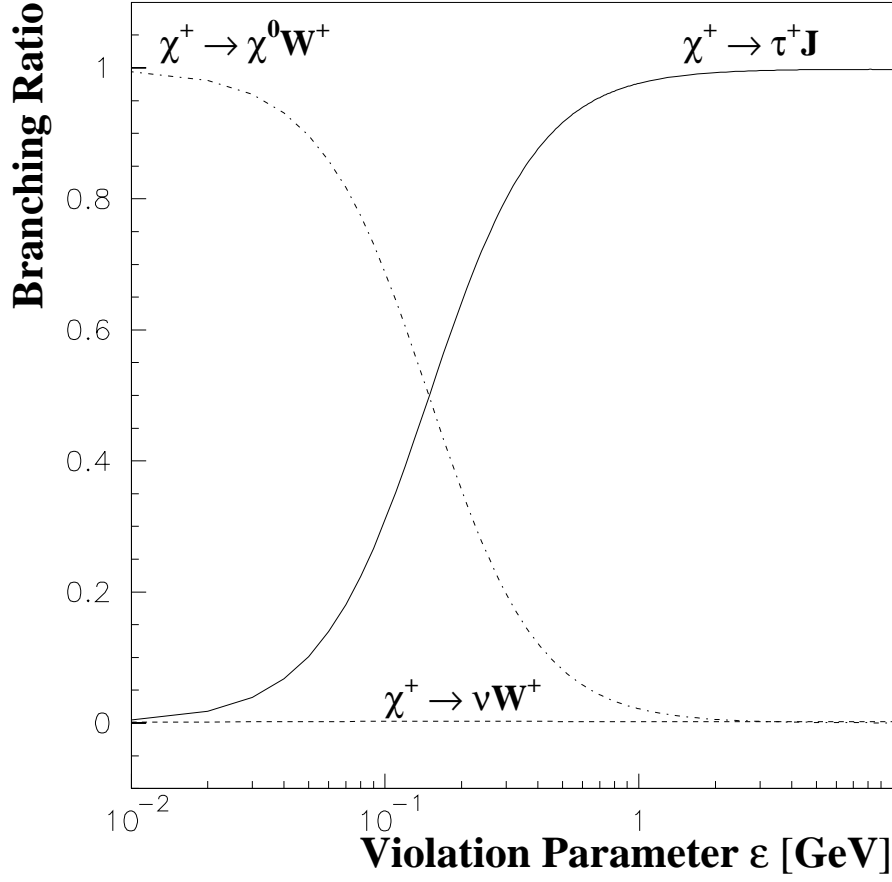
Figure 1: Chargino decay branching ratios as a function of the effective R-parity violation parameter ϵ for $\tan\beta = 2$, $\mu = 100\,\mathrm{GeV/c^2}$ and $\mathrm{M}_2 = 400\,\mathrm{GeV/c^2}$.
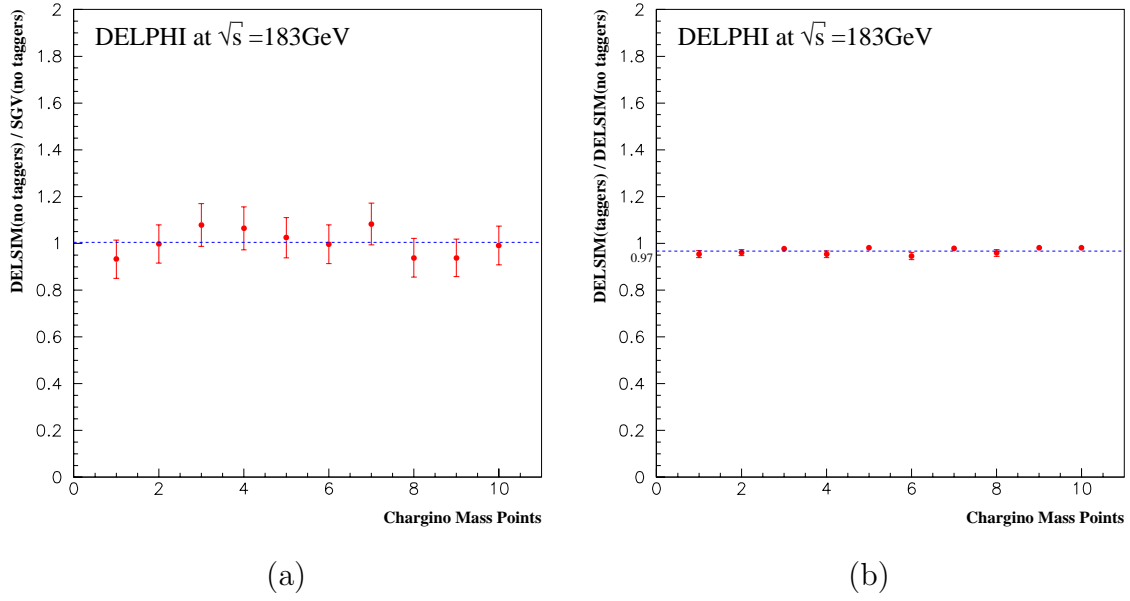
Figure 2: Efficiency correction factors for SGV simulated signals. (a) Selection efficiency ratio between the DELSIM simulated events and the SGV simulated events, if the taggers are not considered in the DELSIM simulated events. (b) Ratio between the selection efficiencies for the DELSIM simulated events with and without the tagger cut. The dashed line shows the average value for the efficiency correction factor that is equal to 1, if we compare DELSIM and SGV efficiencies (a) and equal to 0.97, if we use the tagger cut for the DELSIM simulated events (b).
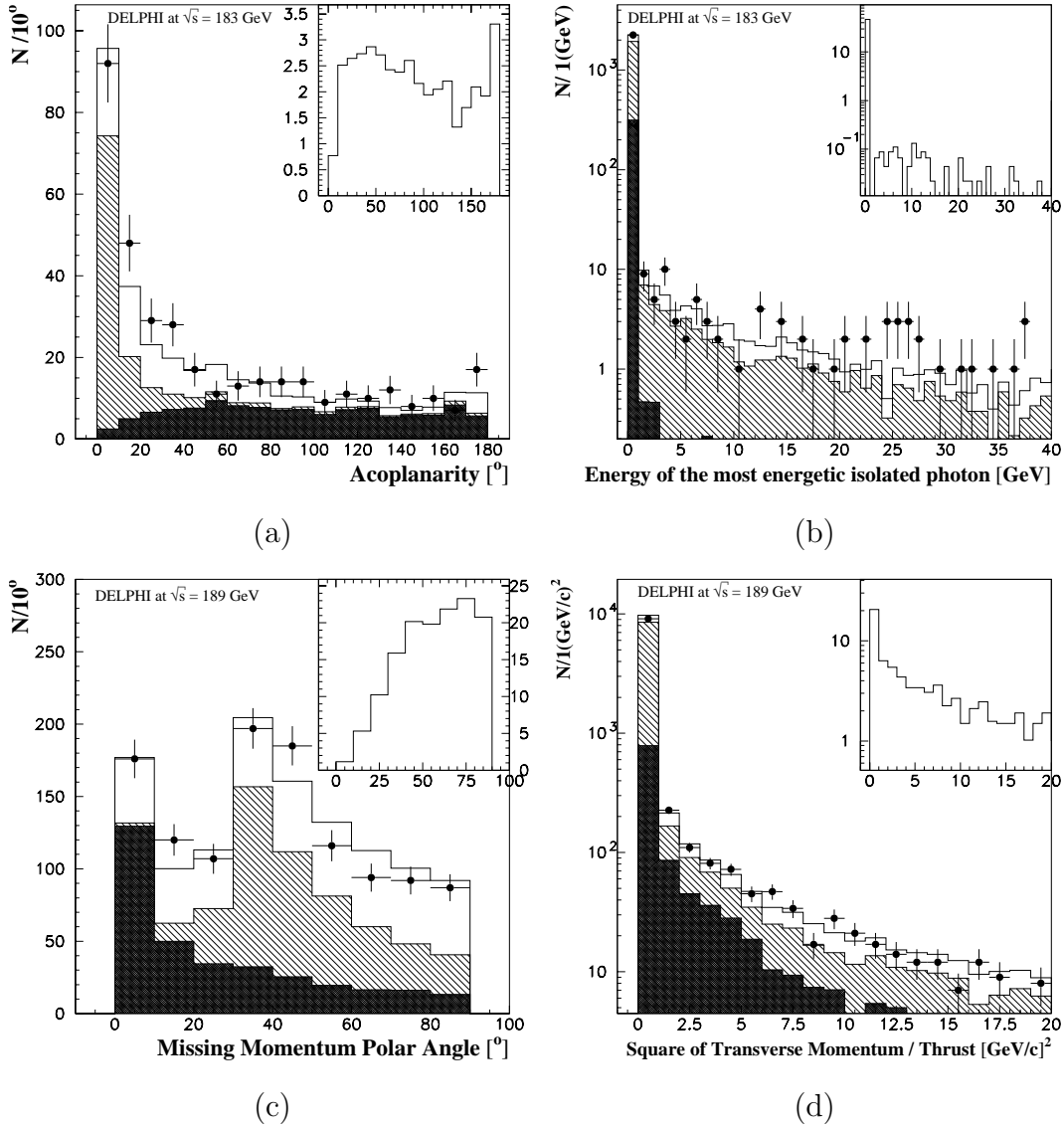
Figure 3: Distribution of (a) acoplanarity, (b) energy of the most energetic isolated photon, (c) angle between the missing momentum and the beam-axis and (d) square of transverse momentum with respect to the thrust axis divided by the thrust, requiring that the events had two clusters of well reconstructed neutral and charged particles, less than 7 charged particles and a total transverse momentum above $4\,\mathrm{GeV/c}$. For the acoplanarity and the missing momentum polar angle distributions it was also required that the square of the transverse momentum with respect to the thrust axis divided by the thrust was above $0.75\,(\mathrm{GeV/c})^2$ and above $1\,(\mathrm{GeV/c})^2$, respectively. The points with error bars show the real data, while the white histograms show the total simulated background. The distributions corresponding to the $\gamma\gamma$ background and the Bhabha scattering are shown as dark and hatched histograms, respectively. An example of the two body decay mode $\tilde{\chi}^{\pm} \to \tau^{\pm} + J$ behaviour for $\tan\beta = 2$, $\mu = 100\,\mathrm{GeV/c}^2$ and $\mathrm{M}_2 = 400\,\mathrm{GeV/c}^2$ is shown in the inserts for each plot.
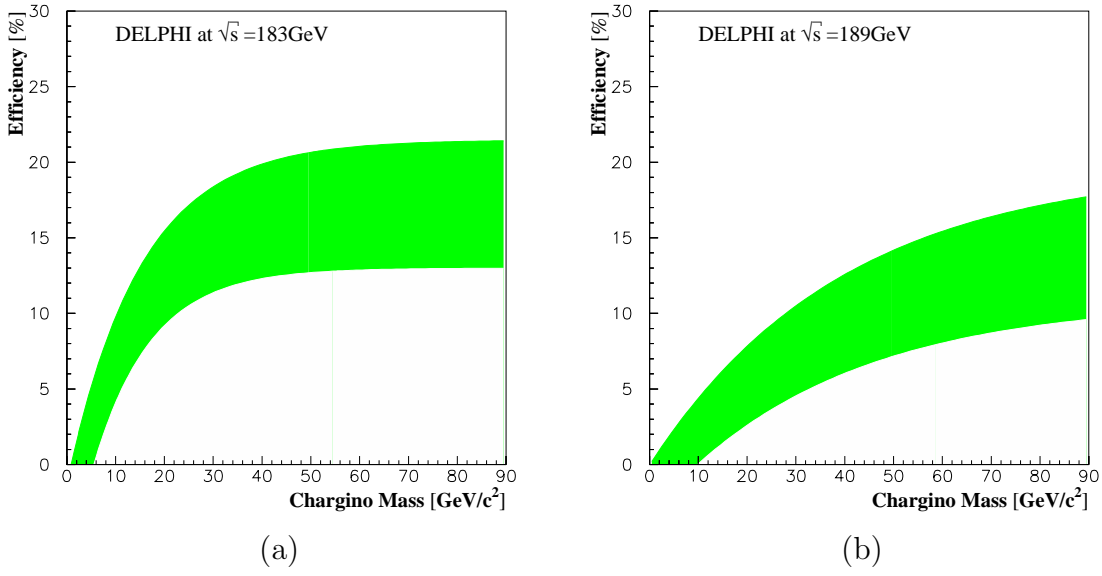
Figure 4: Chargino detection efficiency as a function of the chargino mass for (a) $\sqrt{s} = 183\,\text{GeV}$ and (b) $\sqrt{s} = 189\,\text{GeV}$, considering only the two body decay mode $\tilde{\chi}^{\pm} \to \tau^{\pm} + J$. The bands correspond to the statistical uncertainties combined with the effect of generating events with different MSSM parameters M_2 and μ, which have been varied in the ranges $40\,\text{GeV/c}^2 \leq M_2 \leq 400\,\text{GeV/c}^2$ and $-200\,\text{GeV/c}^2 \leq \mu \leq 200\,\text{GeV/c}^2$, for $\tan\beta = 2$.
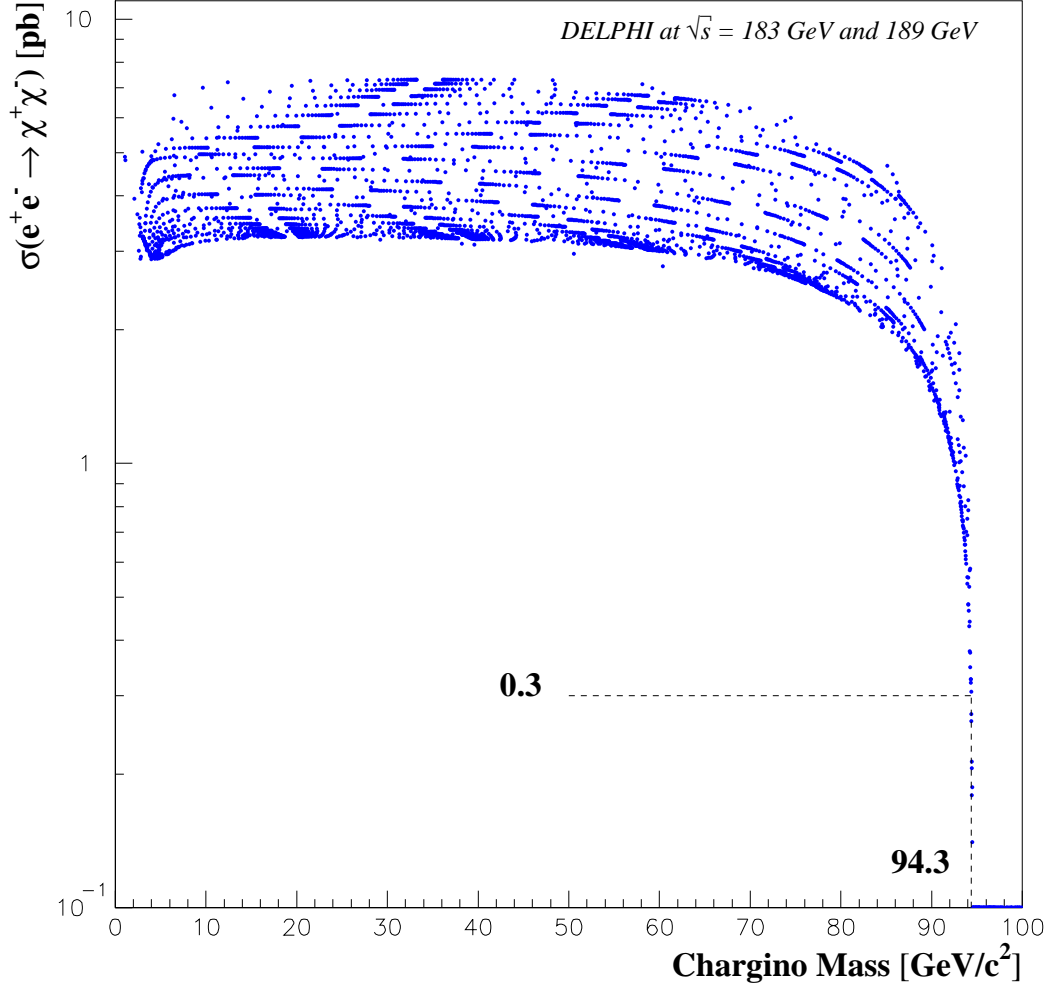
Figure 5: Expected $e^+e- \rightarrow \tilde{\chi}^+\tilde{\chi}^-$ cross-section at $189\,\mathrm{GeV}$ (dots) as a function of the chargino mass, assuming a heavy sneutrino ($M_{\tilde{\nu}} \geq 300\,\mathrm{GeV/c^2}$). The dots correspond to the generated events at different chargino masses for the MSSM parameter ranges: $40\,\mathrm{GeV/c^2} \leq \mathrm{M_2} \leq 400\,\mathrm{GeV/c^2}$, $-200\,\mathrm{GeV/c^2} \leq \mu \leq 200\,\mathrm{GeV/c^2}$ and $2 \leq \tan\beta \leq 40$. At the 95% confidence level, assuming the chargino decays mainly to $\tau^\pm J$, the maximum allowed chargino production cross-section in the excluded mass region is $0.3\,\mathrm{pb}$ and the corresponding lower mass limit is $94.3\,\mathrm{GeV/c^2}$.
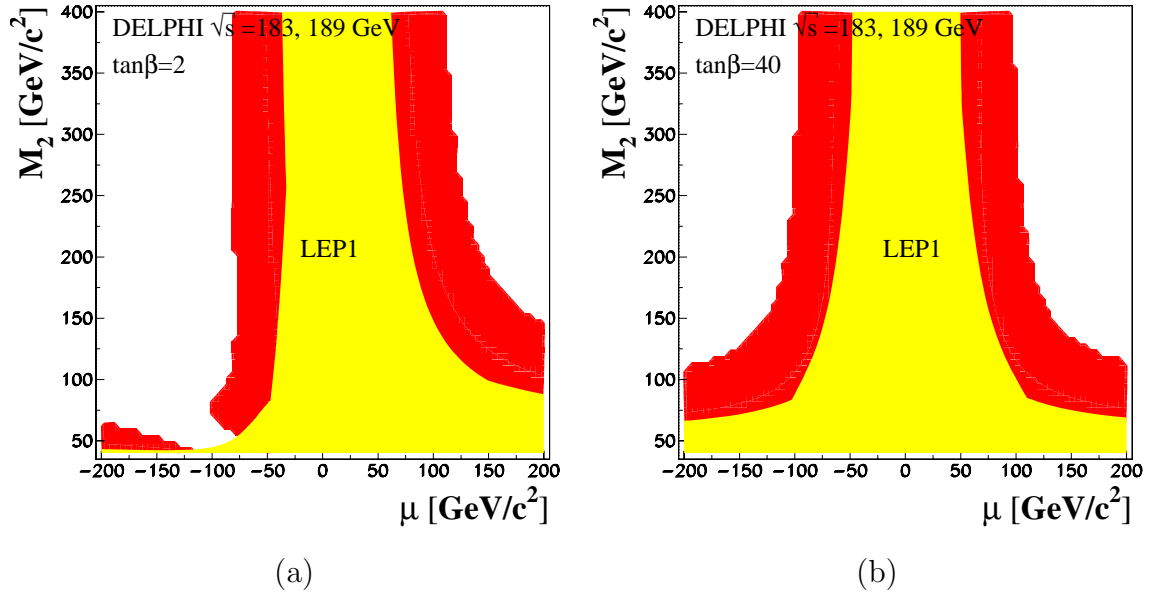
Figure 6: Regions in the μ, M_2 parameter space excluded at the 95% confidence level for (a) $\tan\beta = 2$ and (b) $\tan\beta = 40$, assuming $M_{\tilde{\nu}} \geq 300\,\mathrm{GeV/c^2}$. The exclusion area obtained with the $\tilde{\chi}^{\pm} \to \tau^{\pm} J$ search is shown in dark grey and the corresponding area excluded by the LEP1 data[23] is shown in light grey. The hole seen on plot (a) around $M_2 = 50\,\mathrm{GeV/c^2}$ and $\mu = -120\,\mathrm{GeV/c^2}$ is due to the low branching ratio (below 5%) for the $\tilde{\chi}^{\pm} \to \tau^{\pm} J$.